Piping System Inelastic Calculation During Thermal Shocks Comparison with Experiments

M.N. Berton

C.E.A., CEN Cadarache, DRNR/STRA, B.P. No. 1, F-13115 St. Paul-lez-Durance, France

P. Permezel

Electricité de France, SEPTEN, 12-14 av. Dutrievoz, F-69628 Villeurbanne Cedex, France

Abstract

Accounting for the temperature gradient in the pipe thickness in inelastic calculations has important consequences on the design and analysis of LMFBR piping. The results of the VICTUS test should either qualify or suggest modifications of the existing calculation procedures.

This paper presents the calculations for the first phase of the experimental program : tests on a plane loop subjected to in-plane bending (load controlled) superimposed on thermal shocks. Results given by currently used finite elements codes (3 D shell or special element for pipes) are compared and discussed.

1 Introduction

This paper is a complement of the communication E6/4 (Reference <1>) on the VICTUS test results for expansion loop N° 1 (in-plane loading). The objective here is to compare the calculated predictions with the actual test results, and thus to assess the validity of existing computer codes by comparison with thermal shock tests on piping systems. These codes are designed to take account of the pipe thickness temperature gradient in a plastic calculation.

The thermal shocks sustained by the N° 1 VICTUS loop were therefore computed using a shell code (TRICO) and a special pipe element code (local TEDEL) with two different hardening currently used models : an isotropic model (TEDEL and TRICO) and a linear kinematic model (TRICO only). The results of each calculation will be compared with the test findings.

2 Brief Description of N° 1 Expansion Loop Tests

The tests performed on the N° 1 expansion loop are briefly reviewed here; further details will be found in reference <1>.

2.1 Loading

The N° 1 expansion loop was submitted to a primary load of approximately 1000 daN (Figure 1) that produced in-plane load controlled bending in all four elbows, cold thermal shocks resulting in a 130-150°C temperature gradient in the steel thickness , and then a hot thermal shock are superimposed.

The mean-temperature and equivalent linear thermal gradient curves during shock 1 (cold shock) and shock 10 (hot shock) are showed in figures 4 and 5 of reference <1> (E6/4). This values are calculated from measured sodium temperatures, by a monodimensionnal (cylindrical) thermal conduction code. The heat exchange coefficients are estimated to meet the measured steel skin temperatures.

In this paper, the thermal loading is repeated by the equivalent linear thermal gradient (=$\Delta T1$).

2.2 Geometry

The loop geometry is shown in Figure 1. The mean thicknesses measured ultrasonically were 8.37 mm in the elbows, and 7.71 mm in the straight portions (compared with a design thickness of 8.18 mm).

2.3 Material Characteristics

The loop is made of 316 L stainless steel.

The monotonic tensile loading curves obtained on specimens taken in the lateral part of the elbow are shown in Figure 2.

The residual stresses have not been supressed by heat treatment.

3 Calculation Methods

3.1 Shell Calculation with a Kinematic Hardening Model

The TRICO code from the "CASTEM" (Reference <3>) code system was used with the following characteristics :

- conventional 3-node shell calculation with 7 plasticity integration points in the thickness
- the 3-node shell mesh is shown in Figure 3. Due to geometrical and stress-loading symmetry, only 1/8 of the expansion loop was meshed.
- linear temperature gradient in the thickness
- the material properties are assumed to vary parabolically with the mean shell temperature. Young modulus: $E = 20080. - 4.31t - .892 \times 10^{-2} t^2$ hbars
  coefficient of thermal expansion: $\alpha = (15.77 + .666 \times 10^{-2} t - .296 \times 10^{-5} t^2) \times 10^{-6}$ m/m°C
- bilinear kinematic hardening model (the tensile curves used are plotted in Figure 2).

3.2 Shell Calculation with an Isotropic Hardening Model

The plastic calculation was also performed using the TRICO code. The characteristics were the same as before, except for the isotropic strain hardening model (cf tensile curves in Figure 2). Young modulus and coefficient of thermal expansion are constant :

$$E = 17400 \text{ hbars} \quad - \quad \alpha = 17.7 \times 10^{-6} \text{ m/m°C}$$

3.3 Beam Type Calculation Using Special Pipe Elements with an Isotropic Hardening Model

The "local TEDEL code from the CASTEM system was used; it involves a conventional beam calculation with special pipe elbow elements allowing local plasticity, based on von Karman's theory <2>.

The major characteristics of this method are the following :

- each element of beam mesh correspond exactly to a ring of shell mesh
- 7 plasticity integration points in the tube thickness
- linear temperature gradient in the thickness
- 5 terms taken into account in the Fourier series breakdown (cf <2>) :0,2θ,4θ,6θ,8θ
- material properties variations and isotropic hardening curve similar to the second shell calculation described above (§ 3.2).

4 Results

The most interesting results given by these calculations are presented here.

4.1 Residual Loop End Displacement After the Thermal Shock

The residual displacement was calculated for shock N° 1 (cold), shock N° 2 (cold), and shock N° 10 (hot). As no further plastification was indicated by the calculation for shock N° 2, the remaining cold shocks were not computed (this result was obtained with all three methods). The following table compares the test results with the three calculated predictions.

	RESIDUAL LOOP END DISPLACEMENT (MM)		
	SHOCK 1	SHOCKS 2 TO 7	SHOCK 10
Test value	6.5	3.2	12.5
TRICO-Kinematic	9.5	0	6.2
TRICO-isotropic	10.3	0	10.9
TRICO-isotropic	14.2	0	18.9

A very significant point is thus that none of these codes predicts the thermal ratchetting.

4.2 Loop End Displacement Evolution During the Shocks

Figure 4 compares the experimental and calculated displacements of the free end of the loop for shock 1; Figure 5 compares the same data for shock 10.

4.3 Residual Ovalization

Figures 6 (shock 1) and 7 (shock 10) compare the computed and measured residual ovalization in the four elbows.

The measured ovalization difference in the four elbows is the result of slight dissymmetry in the stress loading.

4.4 Residual stress

The figures 8 to 11 show the residual stress in the most loaded section after shocks 1 and 10 in the internal and external skin of the pipe (equivalent von Mises stress with the sign of the hydrostatic stress).

5 Analysis and Discussion

The most interesting results of this calculation are:

- None of the plasticity models and codes used predicts the measured thermal ratchetting.
- TRICO overestimate the first shock, and underestimate the tenth shock.
- TEDEL overestimate this two shocks.
- The isotropic hardening model seems better that the kinematic one to calculate thoe shock 1 and 10.

The following remarks can explain this results :

- The thermal loading used seems inadequate : it is generally thought that the thermal peak in the shell thickness ($\Delta T2$) has not influence on thermal ratchetting. Well, the influence of this seems determinant to the residual stresses. News calculations with actual thermal loading will show any $\Delta T2$ influence.
- The bilinear kinematic hardening model gives a poor representation of the tensile curve, the isotropic perfectly describes this curve.
- The material characterization was performed in the lateral part of elbow while the maximum plastification for a cold shock occurs in the intrados. It is possible that the material in this area has subjected to greater hardening than in the lateral part, which would account for the better loop resistance to the loading.
- For the "local" TEDEL results, which are rather different from the test findings, it is thought that the determining factor is that no allowance was made for propagation of the ovalization (2θ terms) in the straight portions because the stresses are then overestimated. Moreover the radius of pipe is not small comparatively to the radius of elbow (one of von Karman's hypothesis).
- The TRICO mesh (Figure 3) cannot account for the maximum stress, since the stresses are given for the center of gravity of an element; this explains the slightly underestimated plasticity.
- No allowance was made for residual manufacturing stresses or for thickness variations.

6 Conclusions

The best calculation method to calculate one shock, appears to be TRICO with an isotropic hardening model (except if this result changed in the actual thermal loading calculation).

The use of such a computer code for a complete piping system is obviously out of the question. It was necessary to improve beam type codes such as TEDEL.

None of the calculations performed was able to predict the thermal ratchetting observed. The same calculations will have to be repeated with the actual thermal loading in the thickness ($\Delta T1 + \Delta T2$) and a plasticity model more qualified to account the cyclic plasticity.

The VICTUS tests on the N° 2 expansion loop will involve similar calculations with out of plane bending.

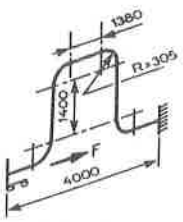

LOADING : F = 1000 daN - ΔT = 130 °C - 150 °C
PIPES DIMENSIONS : Diameter Ø = 219.18 mm
Thickness e = 8.18 mm
Bend's radius R = 305 mm

FIGURE 1 : EXPANSION LOOP N° 1

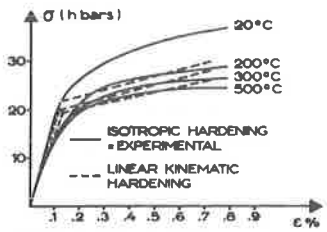

FIGURE 2 : MONOTONIC STRESS-STRAIN CURVES

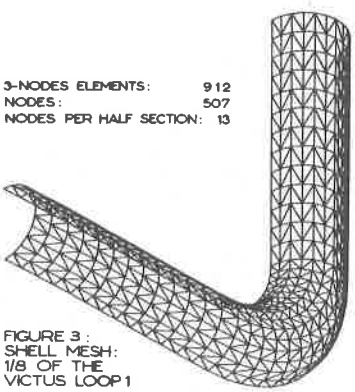

FIGURE 3 : SHELL MESH: 1/8 OF THE VICTUS LOOP 1

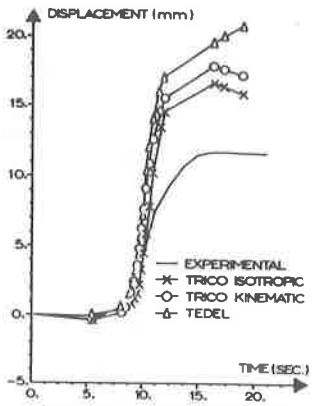

FIGURE 4 : END DISPLACEMENT DURING SHOCK 1

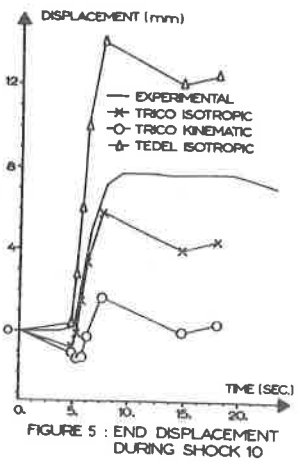

FIGURE 5 : END DISPLACEMENT DURING SHOCK 10

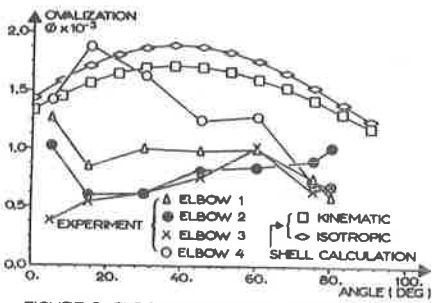

FIGURE 6 : ELBOW'S RESIDUAL OVALIZATION AFTER SHOCK 1. COMPARISON EXPERIMENT - CALCULATION

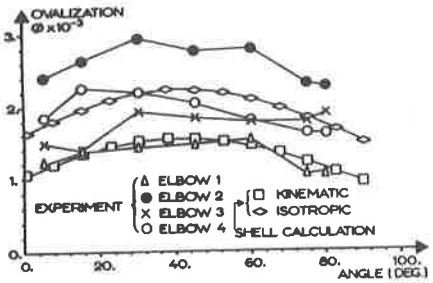

FIGURE 7 : ELBOW'S RESIDUAL OVALIZATION
AFTER SHOCK 10. COMPARISON
EXPERIMENT - CALCULATION

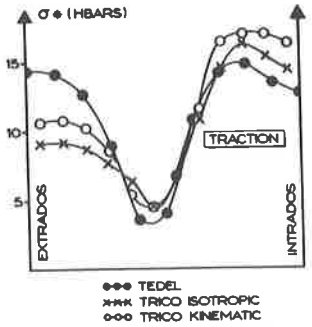

FIGURE 8 : RESIDUAL VON MISES STRESS
AFTER SHOCK 1
MAXIMUM LOADING SECTION
EXTERNAL SKIN

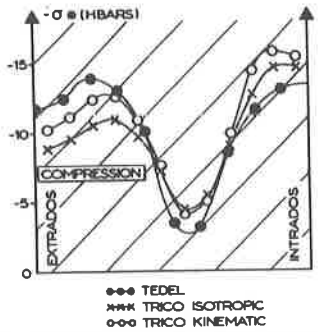

FIGURE 9 : RESIDUAL VON MISES STRESS
AFTER SHOCK 1
MAXIMUM LOADING SECTION
INTERNAL SKIN

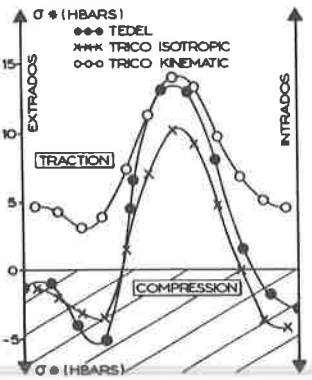

FIGURE 11 : RESIDUAL VON MISES STRESS
AFTER SHOCK 10
MAXIMUM LOADING SECTION
EXTERNAL SKIN

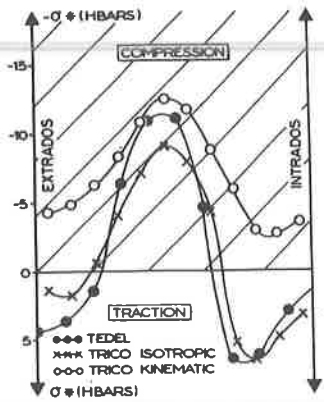

FIGURE 10 : RESIDUAL VON MISES STRESS
AFTER SHOCK 10
MAXIMUM LOADING SECTION
EXTERNAL SKIN